

# TECHNICAL REVIEW

No.20 / September 2023



Technical Review  
MAPNA TURBINE ENGINEERING & MANUFACTURING CO. (TUGA)



Willpower to Empower Generations

# TECHNICAL REVIEW

## Editorial & Production

Editorial Director:

*Jabery, Roohollah*

Associate Editors:

*Rashidi, Saeid*

*Hajizadeh, Hamed*

Coordinator:

*Azizi, Fakhroddin*

Graphic Designer:

*Radfar, Kianoosh*

### **Cover Page:**

Machining the NECK groove of a steam turbine blade in  
MAPNA Turbine

# Editorial

Here at MAPNA Turbine, we are passionately devoted to our continuing quest for innovation and efficiency. Besides our effort to enrich our portfolio of products, we actively explore new techniques and best practices to enhance our products and manufacturing processes so as to achieve a more optimized utilization of resources. It is in this context and with great pleasure that a brief account of a few recent achievements is presented to you, our valuable readers, in this edition of MAPNA Turbine Technical Review.

The first article elaborates on the favorable results of employing the growing field of Additive Manufacturing in production of fuel nozzle tip of heavy-duty gas turbines. Printing this part with the SLM method completely eliminates the need for joining processes and dramatically reduces the buy-to-fly ratio as well as machining time.

The second article provides a prime example of how a simple modification such as a tool replacement can save thousands of hours of machining in a manufacturing process. In this case, the B0.8 tool, used to machine the NECK groove of MST-55C and MST-54C steam turbine blades, was replaced with a dovetail cutting tool which is not conventionally used for this purpose. The result was astonishing as 4500 hours of machining as well as 2500 hours of tool sharpening were saved and the NCRs were reduced to fewer than 30%.

Steps taken to address the challenges caused by an increase in dust amount in the air filtration systems of MAPNA Turbine's mobile power plants are outlined in the third article. The adopted solution constitutes adding pre-filter stages and designing filter houses which successfully facilitated the filter replacement process and reduced the number of required shutdowns for filter replacement from 3 to only 1 per year.

The fourth article reflects on adopting the Inverse Design method as a new valuable approach, enabling more efficient compressor designs based on previous experience. The implementation of this method, coupled with the integration of optimization algorithms and numerical software by MAPNA Turbine design office, represents a significant leap forward in the development of innovative compressor designs such as those incorporated in advanced H-class gas turbines.

The fifth and final article takes an in-depth look into a novel numerical approach to axial compressors simulation, with focus on decrement in computational costs and time while maintaining the highest possible accuracy. The reliability and efficiency of this method were validated, as a comparison made between data extracted from the conventional method and the new approach revealed a 95% decrease in computational costs with a deviation of less than 10% in the results.

Please join us in relishing a detailed account of these subjects in this issue of the Technical Review.

Respectfully,

Roohollah Jabery,

Vice President of Engineering and R&D



MAPNA Turbine Company (TUGA)

September 2023



# Contents

3-7



1

Feasibility Study and Production of Gas Turbine Combustion System Parts Using Additive Manufacturing: Turbine Fuel Nozzle Tip

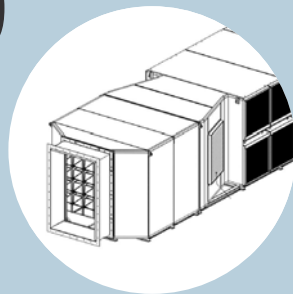
8-15



2

A Modification in Machining the NECK Groove of Steam Turbine Blades

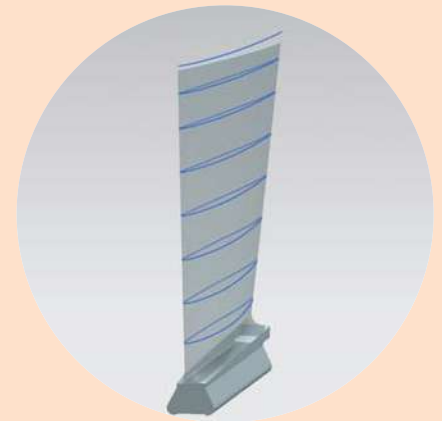
16-20



3

Air Filtration System Upgrade for Mobile Power Plants

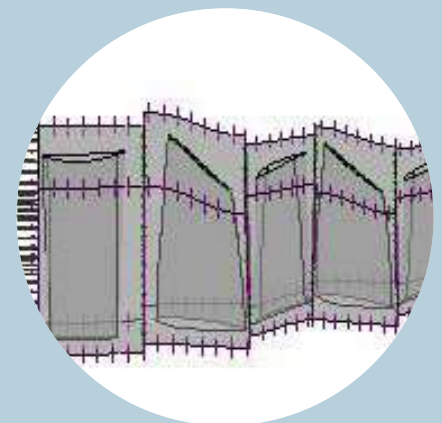
21-28



4

A Novel Approach towards Achieving Optimum Axial Compressor Design

29-32



5

An Innovative Method for Numerical Simulation of Axial Compressors

## Introduction

MAPNA Turbine Engineering and Manufacturing Company (TUGA) has been developing additive manufacturing (AM) technology as a highly efficient and more streamlined manufacturing technique with less raw material consumption; particularly useful for complicated shapes with unique features. In this context, the production of the fuel nozzle tip of a heavy-duty gas turbine was included in the working plan of MAPNA Turbine AM laboratory.

Fuel nozzle tip is a vital component in the combustion system of gas turbines that distributes gas fuel into the reaction zone of the combustion liner to promote a uniform, rapid and complete combustion. In these types of components, the surface roughness of internal (fuel path) channels (incapable to be further machined) plays an important role in fluid flow disturbance prevention.

Formerly, this part was produced by multi-axis machining and subsequent joining process. In the new approach (production by AM), a part consolidation strategy is employed to reduce production steps and time. Furthermore, due to the unique geometry of the aforementioned fuel nozzle tip, the conventional production process requires a high amount of raw material and machining process, entailing a high buy-to-fly ratio (i.e. the ratio of the mass of raw material to the mass of the finished part) which can be significantly decreased through additive manufacturing.



# Feasibility Study and Production of Gas Turbine Combustion System Parts Using Additive Manufacturing: Turbine Fuel Nozzle Tip

Ghodsi, Mahsa  
Aliabadi, Mohsen  
Davarzani, Hossein  
Roozbahani, Behnam

MAPNA Turbine Engineering & Manufacturing Co.  
(TUGA)

## Manufacturing Process Planning and Characterization

Support structures are necessary for selective laser melting process of complicated structures. Among the main jobs of support structures in additively manufactured parts, are maintaining the overhanging areas, resisting deformation caused by thermal stress in the printing process, and heat dissipation from the melt pool to the building platform. Furthermore, the design of support structures greatly affects the printing quality, material consumption, and post-processing time [1].

In the current work, different conventional support structure designs were proposed at the first trial and then optimized to meet the final goal of this project. Utilization of the self-support design method in an optimal manner successfully reduced the amount of material consumption from 21 percent of the whole printed model to 13 percent.

Orientation determination is another essential step in the process planning of AM which directly affects part quality, build time, geometrical tolerance, and fabrication cost. This importance is mainly owed to the layer-by-layer production of parts in AM, which can encounter challenges in inappropriate slopes in the outer wall of the targeted part. In this project, different analysis methods were employed to select the best orientation angle.

Prior to starting the production process, due to the changes in the printed model dictated by support design and selection of optimum orientation, the thermal and mechanical distortions of the fuel nozzle tip were simulated in two steps, first after printing and then after cooling down and build-platform removal (Figure 1). This analysis is crucial for predicting the concentration of thermal and mechanical stresses in the part and particularly the designed supports. Using this simulation, it is also possible to anticipate the separation of the support from the part and the platform and as a result, reduce some risks, such as the collision of the recoater with the part and supports.

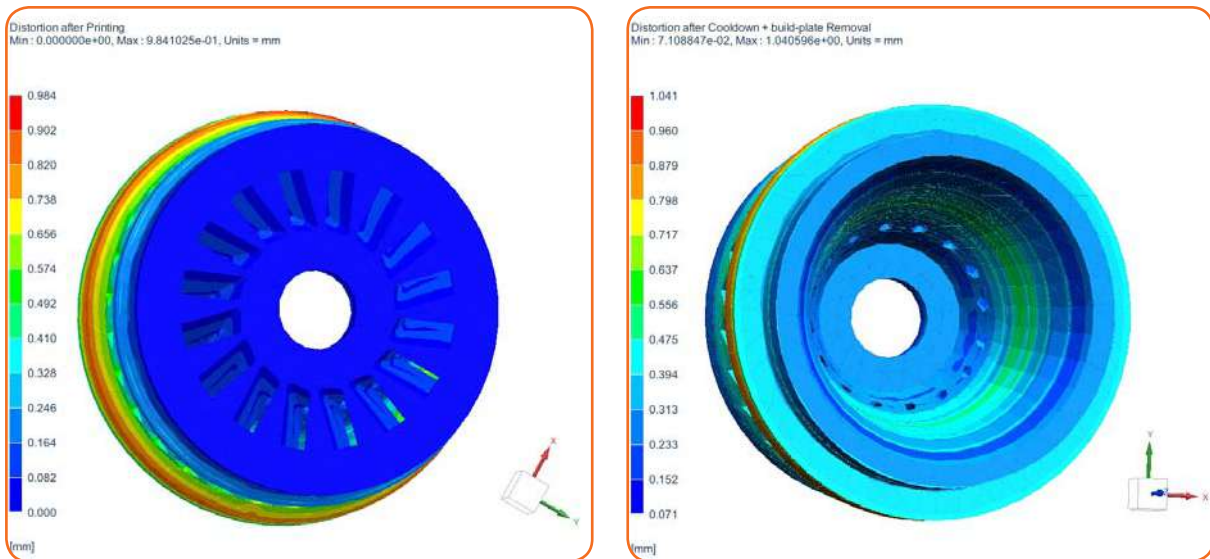


Figure 1- Thermal and mechanical distortion simulation

It is worth mentioning that achieving the desired surface roughness is one of the most critical challenges in the selective laser melting production process. To accomplish a desirable surface roughness, two modifications, namely mesh optimization and changes in process parameters, were made.

Gas-atomized spherical stainless steel 304L powder, with a nominal particle size range of 15 to 53  $\mu\text{m}$ , was used to produce the fuel nozzle tip and nine qualification test samples. All parts were printed by an SLM T300A machine in a purified argon atmosphere using optimal processing parameters. The chemical composition of the used feedstock material and the SLM-printed part are given in Table 1.

Table 1- Chemical composition of feedstock material and final part

Feedstock/Final Part	Powder Chemical Composition (%)							
	C	Mn	P	S	Si	Cr	Ni	Fe
<b>Feedstock material</b>	0.01	1.09	0.022	0.007	0.56	18.92	11.65	Bal.
<b>Final Part</b>	0.02	1.17	-	-	0.6	18.8	11.2	67.7

As a subsequent production step, the building platform was heat treated to achieve various goals such as component stress relief and mechanical properties stabilization. Moreover, as mentioned in the literature, due to extremely high heating and cooling rates during melting and the following solidification process, SLM-built parts have significantly different microstructures compared to conventionally manufactured parts. As a result, the microstructure of AM-built parts tends to be finer, with elongated columnar grains in the building direction. The explained microstructural characteristics lead to material properties anisotropy in different directions.

Overviews of the final (printed and subsequently machined) part and its microstructure are given in Figures 2 and 3, respectively. The porosity percentage analysis of the test sample, which was printed on the same platform, was carried out using the image analysis method. Optical microscopic images were used to accomplish the mentioned goal. To achieve the most accurate results, several cross-sections were studied. Finally, the low value of 0.19 percent was obtained as the percentage of porosity surface fraction in the worst situation.



Figure 2- AM printed and subsequently machined fuel nozzle tip of a heavy-duty gas turbine

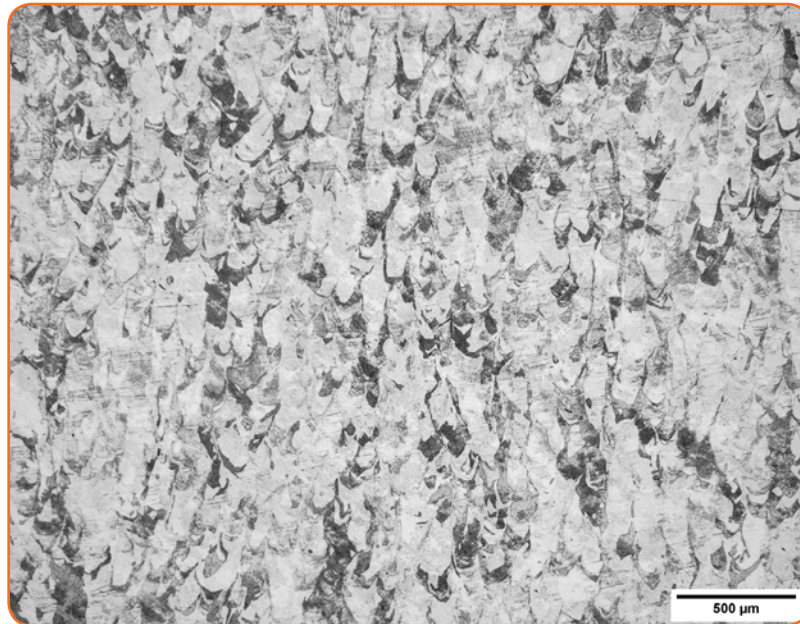


Figure 3- Microstructure of the printed part

According to Figure 3, the part's microstructure is composed of overlapped melted pool tracks with crystallized grains of cellular-columnar structure oriented according to thermal gradient direction. Mechanical properties of qualification samples and standard requirements are presented in Table 2. As can be seen, the additively manufactured part successfully meets the requirements of both ASTM A240 and AMS 5513 standards.

Table 2- Mechanical properties of the additively manufactured part and related standards' requirements

	Sample Orientation	Condition	YS (MPa)	UTS (MPa)	EI (%)	RA (%)	Hardness (HB)
AM Built	Vertical	Stress Relieved	448	602	47	64	190
	Horizontal		476	666	41	59	
ASTM A240	-	-	Min. 170	Min. 485	Min. 40	-	Max. 201
AMS 5513	-	Solution Heat Treated	Min. 207	Min. 517	Min. 40	-	Max.202

The shape complexity of SLM printed parts and micron-scale size of volumetric defects (e.g. cracks, pores, and lack of fusions) cause problems for inspection of these parts via traditional non-destructive testing methods such as ultrasonic and radiographic testing. Indeed, by using the aforementioned inspection techniques, inspecting some sections of the printed component with simpler geometries will be feasible. In this case, the first problem (shape complexity) is solved but only defects with relatively large dimensions (usually more than 300 microns), which are usually not present in such parts, are detectable.

Nowadays, micro-X-ray computed tomography (CT) is used for the evaluation of the volumetric defects in additively manufactured parts. The usage can be attributed to the ability of the process to perform a non-destructive inspection of accessible and non-accessible geometries containing micro-scale features. In addition, the mentioned method is also capable of dimensional assessments and surface topography evaluations. However, it is essential to note that the accuracy of the mentioned evaluations can be limited by the

printed part's geometrical complications [2]. In the present work, due to lack of access to the above technology, just to ascertain the absence of considerable internal defects (which is usually the case with cast parts), the aforementioned traditional radiography test was carried out and no defects were detected. The printed fuel nozzle tip was also inspected using the Fluorescent Penetrant Inspection (FPI) method to evaluate the part from the superficial defects and conditions perspective and no surface-connected defects were detected.

## Concluding Remarks

In this project, the Fuel nozzle tip of a heavy-duty gas turbine was successfully printed using the SLM method. A comparison made between additively manufactured and conventionally produced parts revealed a 64% decrease in the buy-to-fly ratio (that is from 4.2 in conventionally built components at best, to only 1.5 in the SLM printed one). The SLM method also facilitated production process automation. Last but not least, printing the near-net-shape part both reduced the time and amount of machining and eliminated the joining processes required in the conventional approach, which can be expressed as the most significant attainment of this project.

## References

- [1] Jiang, et al. "Support structures for additive manufacturing: a review." *Journal of Manufacturing and Materials Processing* 2.4 (2018): 64.
- [2] Zanini, et al. "X-ray computed tomography for metal additive manufacturing: challenges and solutions for accuracy enhancement." *Procedia Cirp* 75 (2018): 114-118.

# 2

## A Modification in Machining the NECK Groove of Steam Turbine Blades

Aghlmand, Saeed  
Moradi, Shahab

MAPNA Turbine Engineering & Manufacturing Co.  
(TUGA)

### Introduction

One of the most important steps in planning machining operations such as milling, is choosing the optimal machining parameters and proper tools to achieve greater material removal rate, higher quality index, lower costs, and minimum tool wear.

In the manufacturing process of MST-55C and MST-54C steam turbines, a great number of CNC machines on the premises at MAPNA Turbine are dedicated to producing stationary blades. This explains the need for continuous modifications to machining operations where possible. In this context, the NECK groove machining process, with its low machining speed and lack of proper quality, was identified as a critical parameter in the machining of stationary blades.

The present study outlines the geometry of the NECK groove in the aforementioned turbine blades, elaborates on the challenges with the tool formerly used for this machining process, and introduces a more efficient tool to carry out the task.

## The NECK Groove Geometry and B0.8

As shown in Figure 1, the geometry of the NECK groove consists of two connected surfaces with an edge radius of 0.4(mm) and curvature around the turbine axis surfaces. Consequently, the surface of the groove is cylindrical on the wall and conical at the bottom.

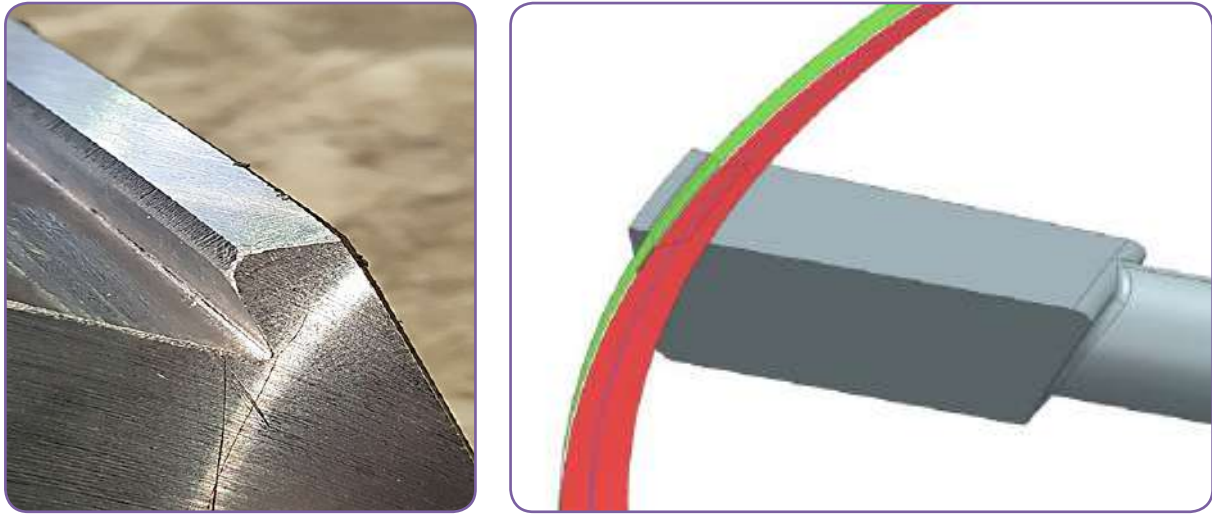


Figure 1- The geometry of the NECK groove and its surfaces

As can be seen in Figure 2, the line resulting from the intersection of the vertical surface of the groove and the middle plane is determined as the longitudinal reference line in the drawing; and all other dimensions of the part are measured relative to it. As a result, the manufacturing process of this groove has to be amply repeatable.

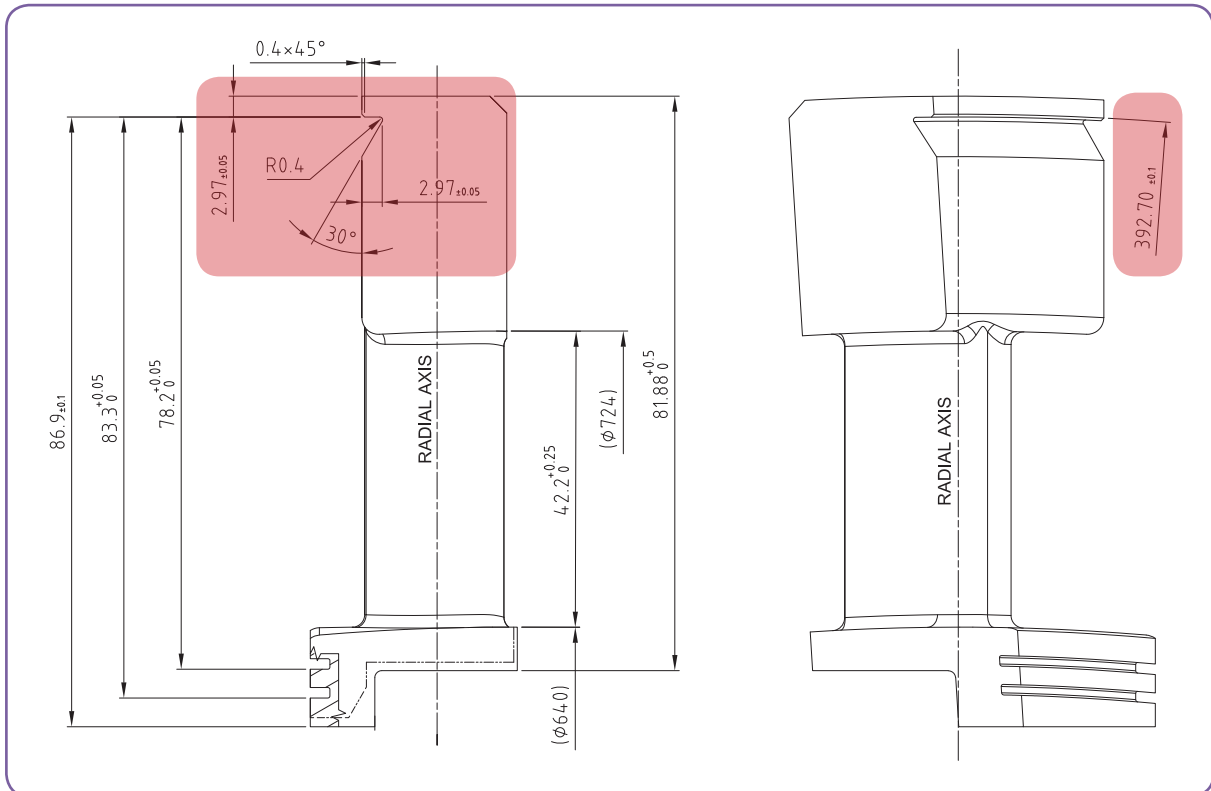


Figure 2- Design tolerance for HPV<sup>1</sup> blades of MST-55C steam turbine

<sup>1</sup>HPV, IPV, and LPV stand for High Pressure Vane, Intermediate Pressure Vane and Low Pressure Vane, respectively.

The most important factor affecting machinability is the cutting tool. Without using the right tool, even if all other variables are carefully controlled, the efficiency of machining operations will be very low.

Figure 3 demonstrates B0.8, the ball nose tool formerly used for machining the NECK groove of MST-55C turbine stator blades. Besides the tool length that increased the unwanted vibrations, the tip diameter of 0.8 mm and the weakness of the tool in terms of geometry, imposed severe limitations on machining parameters and entailed low machining speed and high depreciation rate. As an example, this tool carried out the machining of the floor and wall surfaces separately (Figure 4) which increased the machining time. Furthermore, to control the critical parameters and avoid diffusion, the cutting speed and feed rate were set to the lowest possible values. However, the grooved surfaces were not in the best condition in terms of surface and dimensional quality, and caused an increase in the number of non-conformity reports (NCRs). The B0.8 tool was capable of machining an average of 4 blades in the roughing stage and 2 blades in the finishing stage after each sharpening. As a result, the tool-making department was maximally occupied with sharpening and producing B0.8 tools. Taking everything into account, this tool was labeled as uneconomical, and its replacement was put on the agenda.

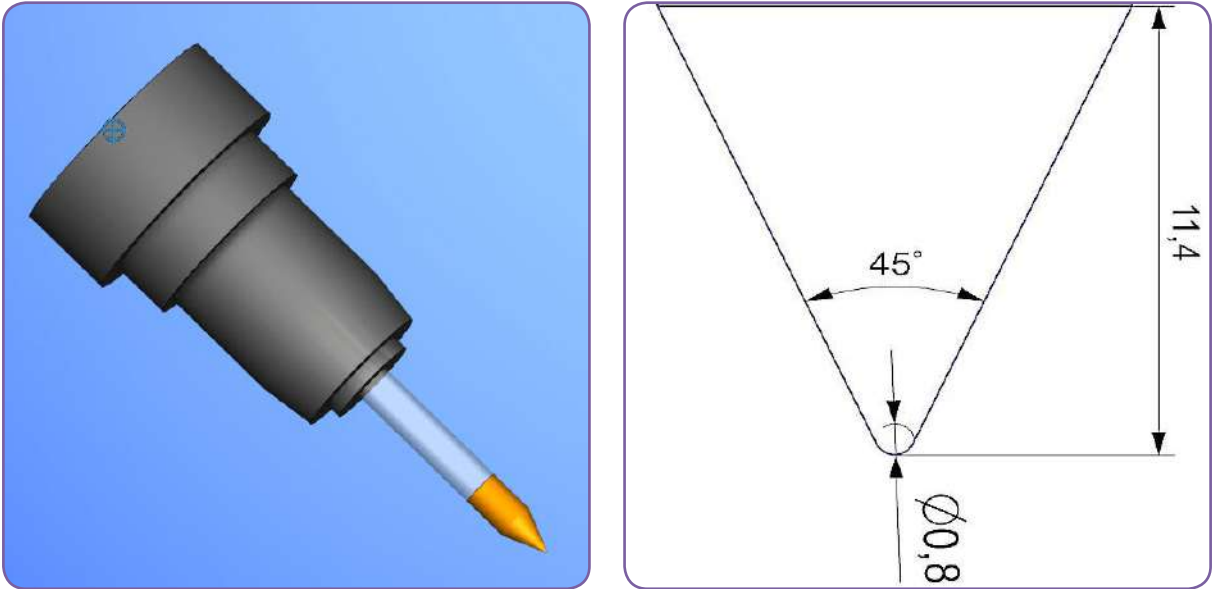


Figure 3- The geometry of the B0.8

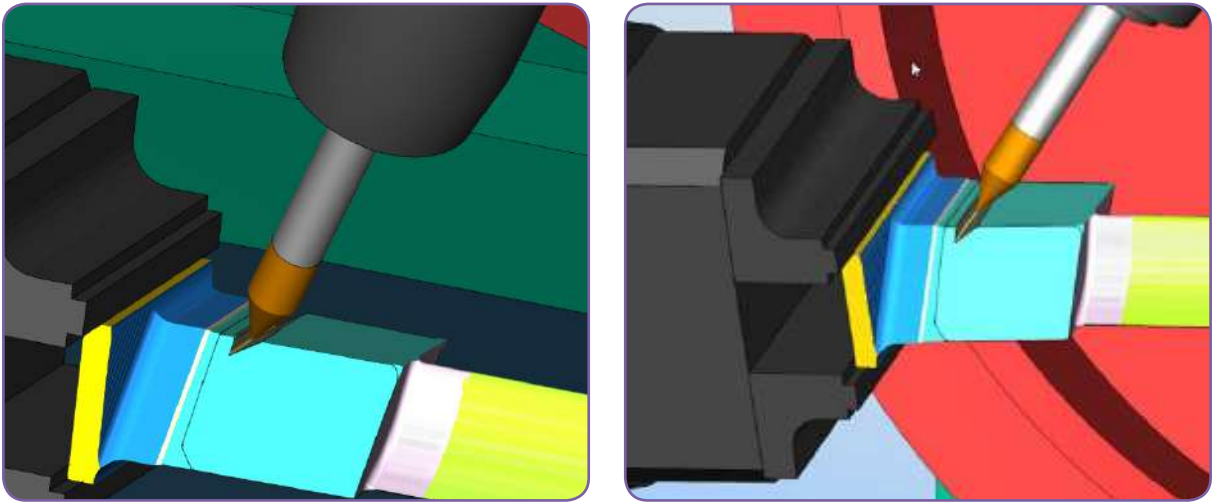


Figure 4- Machining simulation of the bottom (conical) and wall (cylindrical) surfaces of the NECK groove with the B0.8 tool

## The Solution

As it was not possible to use a larger diameter Ball Nose inside the groove, other possible alternatives were considered to replace the B0.8 tool. At first glance, dovetail tools may not seem to be the solution as they are not generally used to create curved grooves and are typically used for straight paths such as Guide Rails (Figure 5). At a closer inspection, it was surmised that a dovetail tool, when used in a five-axis CNC machine, might be able to carry out the task. However, as the tool has to be located at a negative angle in relation to the part, the process might fail due to unwanted contact between the tool and the part.

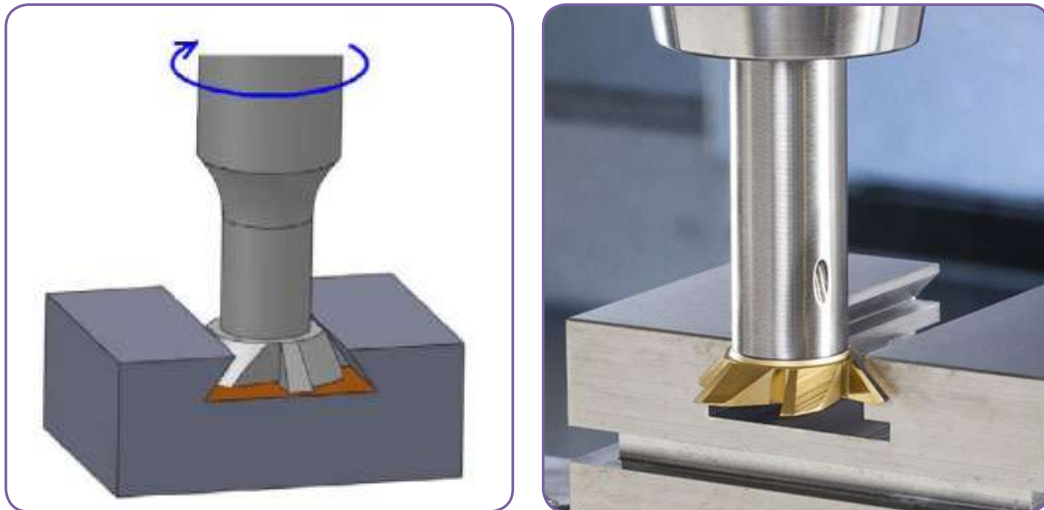


Figure 5- Dovetail tool and features created in its general application

Another factor to be taken into account was that the tool was supposed to machine the wall (cylindrical) and the bottom (conical) surfaces at the same time.

In contrast to the single contact area between two common objects, dovetail milling cutters commonly have more than two contact points between the cutter and the workpiece. The design of the cutter profile also affects the contact patches. It is difficult to theoretically predict the contact area between the cutter and the workpiece [1].

Eventually, the dovetail tool shown in Figure 6 was designed and manufactured to be tested with a 30-degree taper angle and a corner radius of 0.4mm.

The ability to use larger diameters as well as sufficient stiffness to apply optimum values for the cutting parameters were considered the most important advantages of this tool. The increase in the number of cutting edges caused the machining force to be divided among the teeth of the tool which in turn enabled using a higher cutting speed and feed rate.

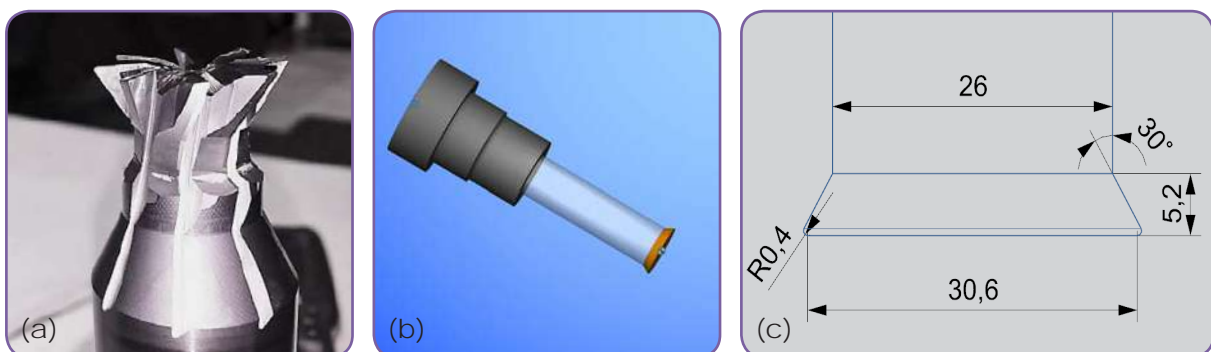


Figure 6- (a) The image of the Dovetail tool (b) The geometry of the Dovetail tool (c) The schematic of the Dovetail tool in simulation

To ensure that the Dovetail tool could be used to machine the NECK groove, the cutting procedure was simulated in a software. The simulation proved that the tool would carry out the task without any unwanted contact when used on a five-axis CNC machine.

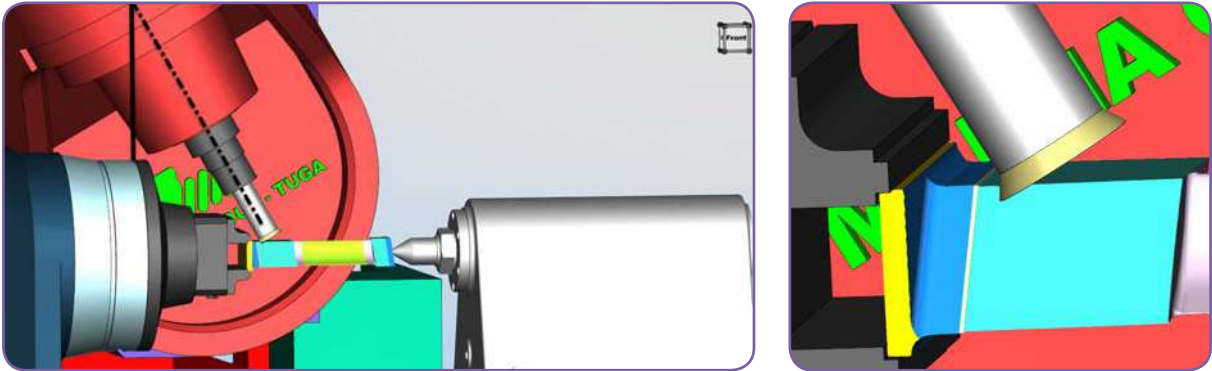


Figure 7- Simulation of NECK groove machining process with Dovetail tool on OMV-800 machine

Table 1 shows the output data from the post-processor for groove machining. The change in the value of all parameters is an indication of the CNC utilizing all its five axes.

Table 1- The output parameters of the Dovetail toolpath program

line	Post processor out-put				
Co-ordinates	X	Y	Z	A	B
1	169.4387	-55.3741	29.9189	181.6485	-29.9589
2	169.2060	-50.5527	29.6331	181.4846	-29.9667
3	168.9976	-45.7292	29.3752	181.3205	-29.9736
4	168.8136	-40.9036	29.1450	181.1564	-29.9798
5	168.6540	-36.0764	28.9426	180.9923	-29.9851
6	168.5187	-31.2476	28.7681	180.8281	-29.9896
7	168.4079	-26.4175	28.6215	180.6639	-29.9933

### Comparison of Machining Results with Dovetail and B0.8 Tool

In this section, a comparison of the developed Dovetail tool and B0.8 shall be made in terms of machining time, production quality, and tool supply cost.

#### ■ Machining Time

Table 2 lists the operations carried out for groove machining of the stator vane stage 26 of the MST-55C steam turbine for both B0.8 and Dovetail tools, along with the actual time of each operation and the total time. According to the table, NECK groove machining with B0.8 takes 40 minutes and shapes up nearly 20% of the blade's total machining time. On the other hand, this procedure takes only 1 minute with the Dovetail tool which is merely 1% of the total machining time. This means that using the Dovetail tool has almost completely removed the machining time of the NECK groove from the list of parameters affecting the total machining time.

Table 2- Comparison of NECK groove machining time in stator vane stage 26 of the MST-55C turbine for B0.8 and Dovetail tool

Operation	Time (B0.8)	Time (Dovetail)
Roughing (1)	00:00:55	00:00:10
Roughing (2)	00:30:32	00:00:10
Pre Finishing	00:06:15	00:00:10
Finishing	00:02:34	00:00:30
<b>Neck Machining (Total)</b>	<b>00:40:16</b>	<b>00:01:00</b>
<b>Blade Machining (Total)</b>	<b>03:22:26</b>	<b>02:43:10</b>

Taking into account the 3000 HPV blades for the MST-55C turbine and a total of 4000 HPV, IPV, and LPV blades for the MST-54C turbine, the NECK groove has to be machined on 7000 blades. Considering a 40-minute reduction in groove machining time on average, the total machining time for the groove has been reduced from 4666 hours to merely 116 hours after replacing the B0.8 with the Dovetail tool (Figure 8).

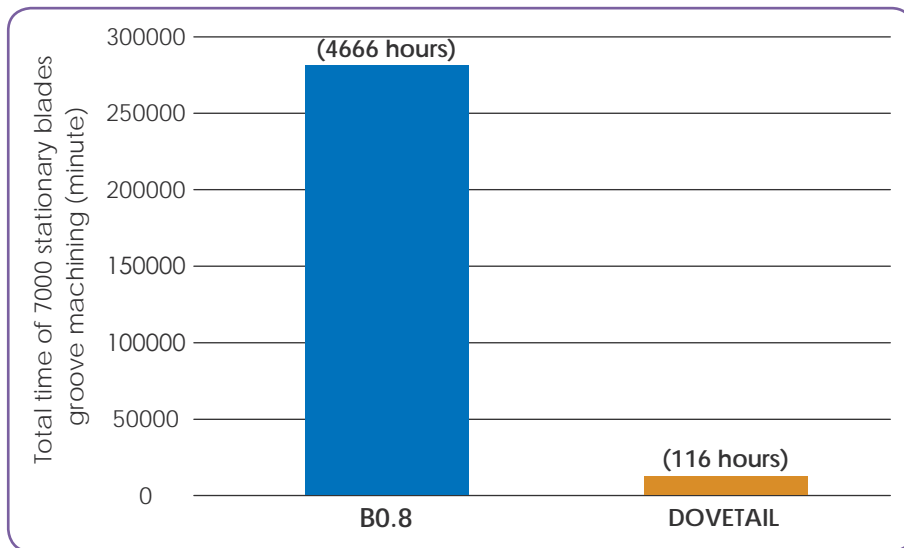


Figure 8- Groove machining time for all MST-55C and MST-54C stationary blades with B0.8 and Dovetail tools

### ■ Production Quality

In the production process, Geometric Dimensioning and Tolerancing (GD&T) should be checked and reported according to the final drawing. As a result, the quality of the blades produced needs to be examined and compared in terms of surface roughness and dimensional quality.

Smart selection of machining parameters such as feed rate, spindle speed, tool radius, and cutting depth can reduce the surface roughness of the part. Considering the delicacy of B0.8 tool geometry, tool vibration was one of the key factors reducing surface quality as it would cause 'tool jumps' leaving some material uncut. This uncut material was responsible for surface roughness variation. Figure 9 shows the effect of changing the tool on improving the smoothness of the groove surface. Figure 10 illustrates the improvement in the dimensional

quality of the NECK groove following the deployment of the dovetail tool instead of the B0.8 tool. In this diagram, the number of non-conformity reports in the various HPV stages of the MST-55C turbine is indicated. According to this diagram, the number of non-conforming blades caused by the deviation of the NECK size from the allowable range was reduced by nearly 70% after the tool was changed.

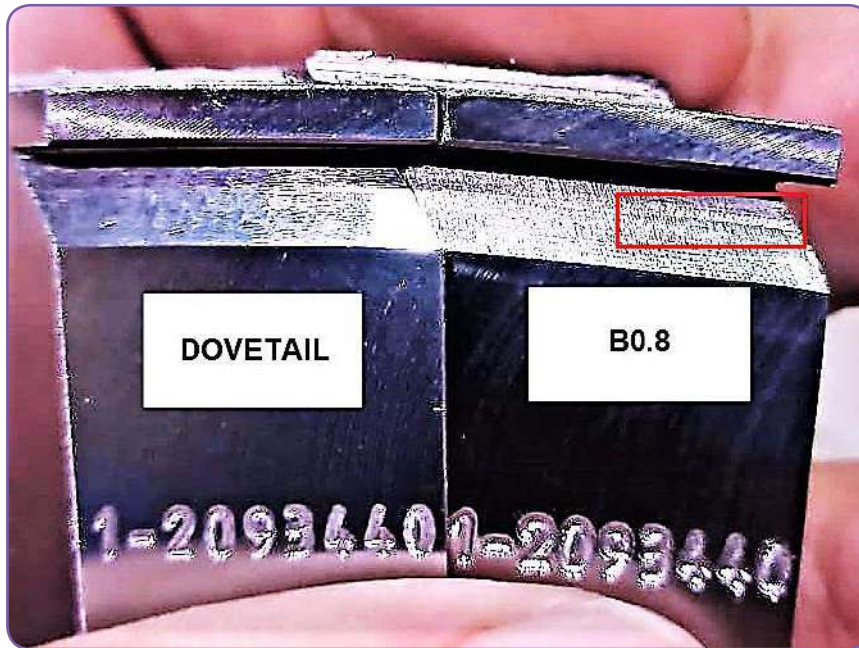


Figure 9- Comparison of surface roughness created in machining with B0.8 and Dovetail tools

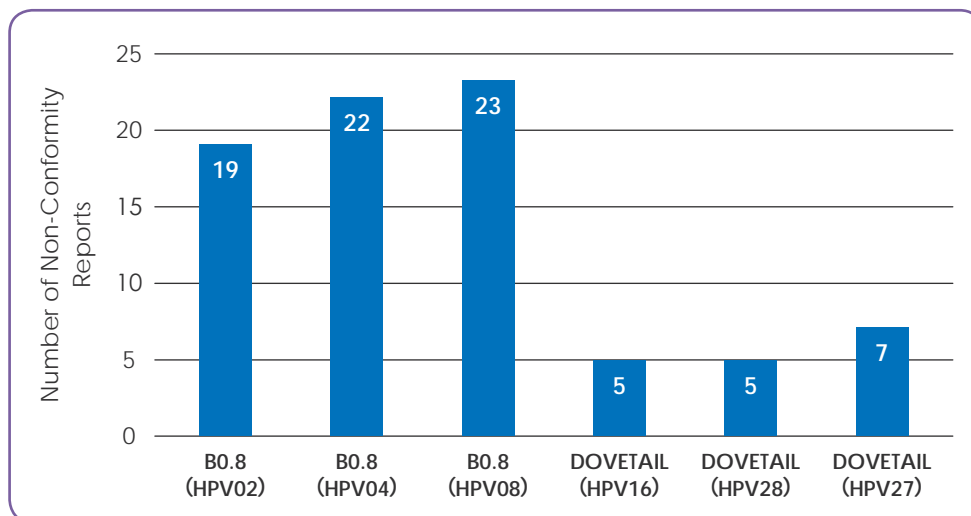


Figure 10- The number of NCRs in various stages caused by the dimensional quality of the groove after machining with Dovetail and B0.8

### ■ Cutting Tool Cost

The complexity of the tool's geometry and dimensional precision have a considerable impact on the cost of manufacturing the tool. On the other hand, the weakness of the tool geometry accelerates its wear, necessitating more frequent sharpening of the cutting edges. Due to the delicacy of B0.8 geometry, the sharpening process, carried out in MAPNA Turbine by the HAWEMAT machine, entailed special challenges. For instance, reaching the required tip radius highly depended on the quality of the sharpening stone wheel, which occasionally made it an

unreasonably long process. As mentioned before, the production reports indicated that each of the B0.8 tools machined an average of 4 blades in the roughing stage and only 2 blades in the finishing stage at their best, before needing to be sharpened. Although sharpening the Dovetail tool takes twice the time needed for that of B0.8 (60 and 30 minutes respectively), in machining 100 stationary MST-55C turbine blades, the B0.8 tool needed to be sharpened 75 times on average; which is much more than only 2 sharpening rounds needed for the Dovetail tool.

Considering the 7000 stationary blades required for MST-55C and MST-54C steam turbines, the total time spent for sharpening B0.8 and Dovetail tools in the case of machining with each of them would add up to 2650 and 140 hours respectively.

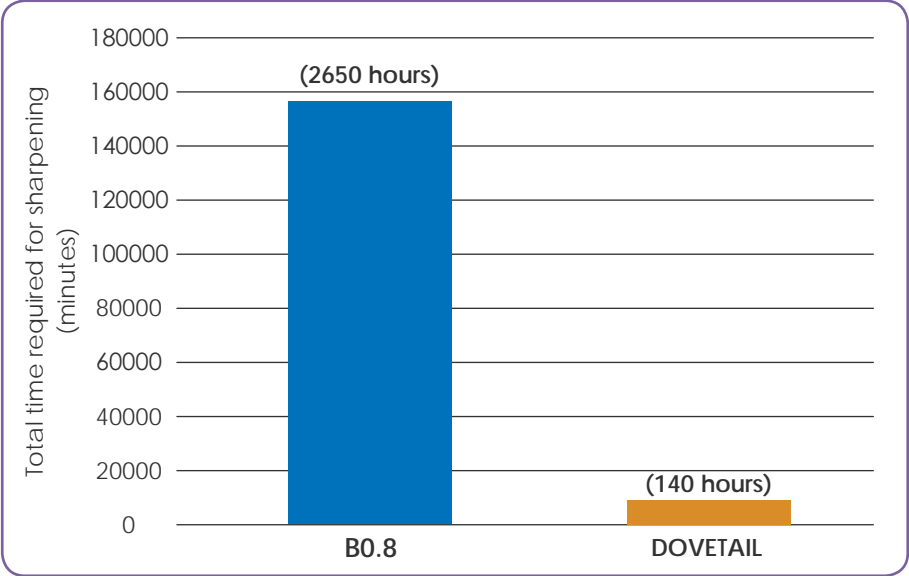


Figure 11- The total time required for sharpening all tools for machining 7000 stationary blade grooves

### Concluding Remarks

To further optimize the machining operations performed on MST-55C and MST-54C steam turbine blades in MAPNA Turbine, a thorough investigation of machining operations was carried out which resulted in the replacement of the B0.8 tool formerly used for machining the NECK groove of the blades, with a more efficient Dovetail tool. In this article, the disadvantages of B0.8 were mentioned, and the desirable results brought about by the replacement were outlined in terms of reduced machining time, improved quality, and diminished cost of tool supply.

A comparison made between the reports before and after the replacement in the manufacturing process of 7000 blades demonstrated a reduction of more than 4500 hours in machining time, a 70% decrease in the number of NCRs, and 2500 hours saved in tool sharpening. Other benefits such as reduction in material cost needed for tool manufacturing were not included.

Although machining with the Dovetail tool has challenges of its own, it has eliminated the problems posed by B0.8 and has successfully turned the NECK groove machining into a stable process.

### References

[1] Yao C.W. et al, "Measurement of the contact area of a dovetail milling cutter using an ultrasonic method" (2013).

# 3

## Air Filtration System Upgrade for Mobile Power Plants

Mollaei, Fouad  
Sobhanifar, Mohammad

*MAPNA Turbine Engineering & Manufacturing Co.  
(TUGA)*

### Introduction

Air filtration is an inseparable part of power plants, reducing the amount of airborne particles in the air prior to its use in the systems. The amount and type of these particles vary greatly depending on the plant environment. Dust is the most unwelcome constituent of these airborne particles as its mechanical properties inflict serious damage on the systems. For instance, it can cause damage to rotating and sealing parts in case of collision at high velocities. Various reports on the damages inflicted by dust particles have turned dust content into one of the main metrics in evaluation of the air quality.

Gas turbine (GT) breathing air filtration is an example of air filters at work. GT consists of rotors and stators conveying air at high speed. As the density of airborne particles is relatively higher than the air, any change in the direction of the stream leads to the impact of the heavier particles on the liners (i.e. air-path boundaries). This impact entails material removal from solid surfaces which can dramatically change the aerodynamic behavior of the moving and stationary parts. This change may result in unsteady and increasing vibrations that may lead to catastrophes like blade-loss which have great consequences in terms of cost and time.

The present study focuses on the challenges caused by increase in dust amount in air filtration systems of MAPNA Turbine's mobile power plants and the solution adopted to minimize the impact. The popular MGT-30 Gas Turbine used in mobile power plants requires air quality corresponding to F9 class according to EN 779.

## As-is Condition

The increase in dust amount in the southwest of Iran during recent years has posed serious challenges to air filtration systems of power plants. A 4-chassis-mounted power plant (4C) with single-stage F9 filtration, and a trailer-mounted power plant (6T) with two filter stages (G4 pre-filters and F9 fine filters) are among the affected sites. These power plants are facing problems such as shortened replacement intervals and pressure drops in filtration stages. Other matters such as the challenging replacement procedure of the pre-filter module in 6T power plant should also be noted.

The air intake system of 4C plant is mounted atop of the GT's centerline level. As a result, the filter house is mounted on a dedicated structure. The schematic of the as-is air intake system is provided in Figure 1. Two triangular shapes at the uppermost left of the image are two weather hoods, tasked with stopping direct rain, birds, and insects from entering the system. There also exists a droplet separator stage before filtering.

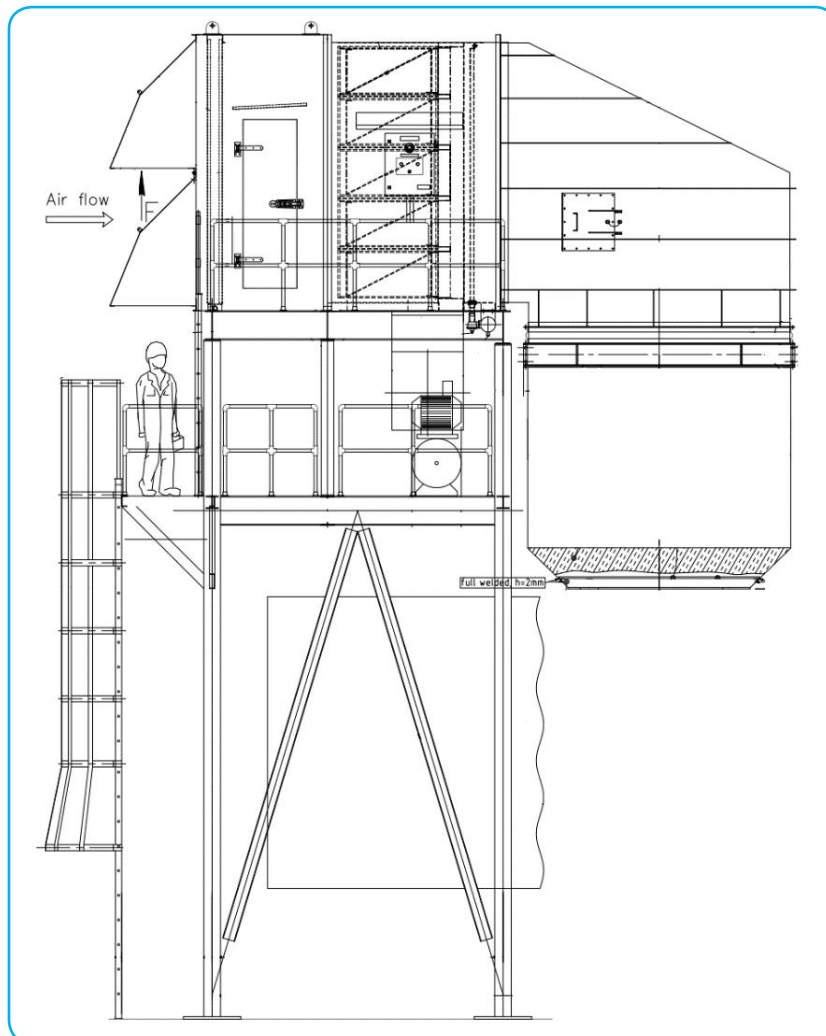


Figure 1- Configuration of the air intake system of 4C plant

The configuration of the air intake system in the 6T power plant is also presented in Figure 2. Pre-filter replacement of this system is a problematic procedure needing a special crane to remove filter holder elements.

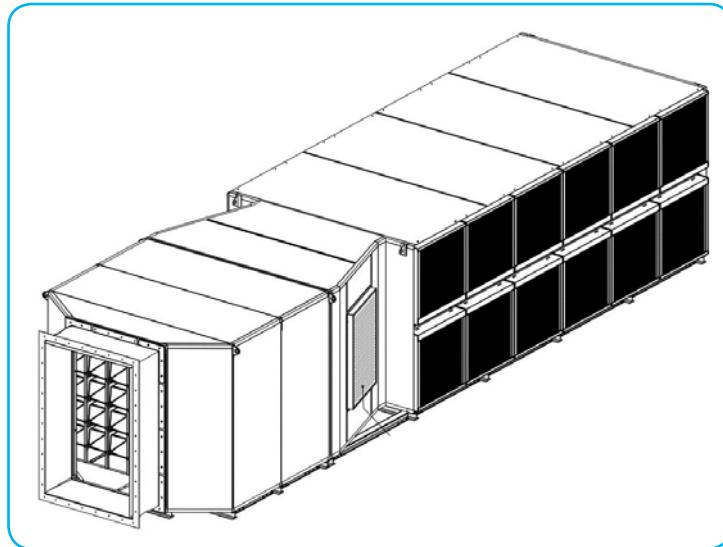


Figure 2- 6T air intake schematics

## Modifications

To further improve the air intake system of 4C plant, an extra filtration stage is designed. This new stage includes G4 pre-filters. The droplet separator stage and weather hoods are moved to the entrance like before. To choose appropriate filters, the datasheet of elements had to be studied closely and main variables such as air mass flow rate of each filter, dust capacity, as well as pressure drop of the filters had to be extracted so that the internal configuration of the new module could be designed. The isometric schematics of the pre-filter module of 4C plant are provided in Figure 3.

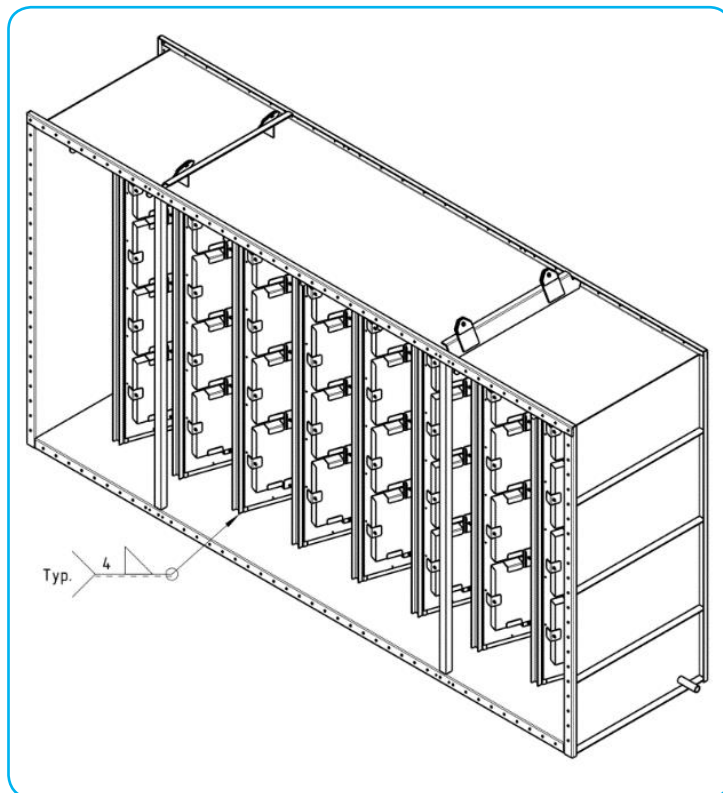


Figure 3- Pre-filter module for 4C

The main advantage of adding a pre-filter stage is its effect on the downtime of the site. The pre-filter stage greatly reduces dust load at fine filters, extending the lifetime of fine filters from 3 months to a year. On the other hand, there is no need to turn the unit off in order to replace the pre-filters; meaning that compared to the three shutdowns needed to change the filters when pre-filters were not in the design, only one shutdown is needed when they are present.

As for the 6T plant, to overcome the filter replacement challenge, it was decided to create a service gallery between fine filters and pre-filters. To do so, a box-like compartment is designed to be installed at each side of the air intake system. The new compartment also provides weather hoods and the droplet separator that were absent in the original design. The final configuration of the pre-filter module is also provided in Figure 4.

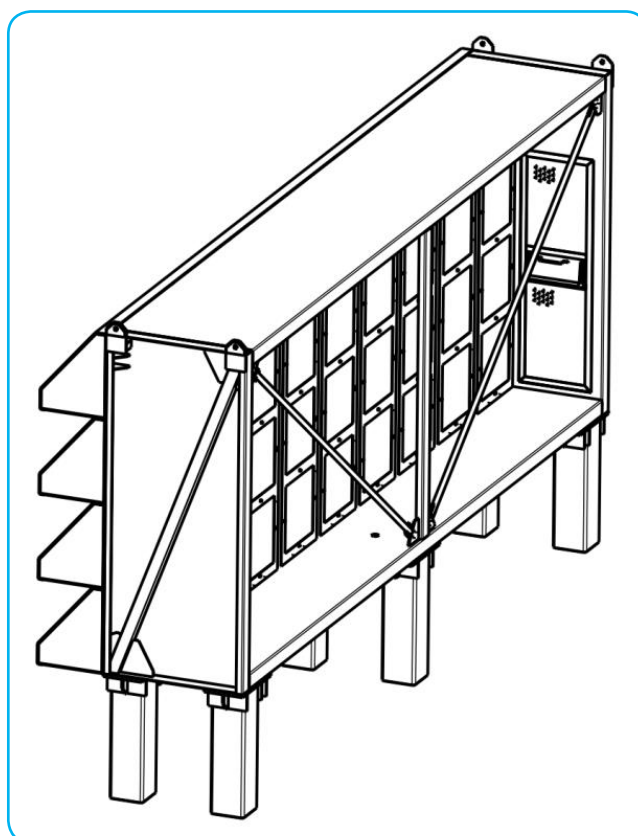


Figure 4: Pre-filter module of 6T plant

## Structural Adaptation and Analysis

To complete the design process, structural analysis of the new configurations had to be carried out and the structures had to be modified to bear the loadings. The load and stress distribution in the new modules were calculated using FEM analysis to check whether they withstood the loading or failed at a certain point(s). According to the contracts of each power plant, national structural and civil standards like the "2800 Iranian National Structural Standard" are to be met.

Loadings required were presented as "Load Cases" that combined various types of excitations, e.g., wind, seismic load, snow, etc. Each of these loads has its own specific guidelines. A combined FEA model was created for each of the new modules to ensure its capability of bearing possible loadings. Apart from stress distribution in the filter modules, the supporting structure also has to be checked structurally. The latter is carried out using standard commercial software.

## Concluding Remarks

This study outlined the details of modifications made to air filtration systems of a 6T and a 4C power plant working in severe weather conditions in terms of dust content.

The main aim of these modifications was to extend the lifetime of fine (F9) filters in order to reduce the number of shutdowns needed to replace them. As a result, it was decided to add a pre-filtration stage to the 4C air intake system. On the other hand, although the 6T plant was already benefiting from a pre-filter stage, a time-consuming and expensive procedure used to be endured to replace its filters. Therefore, a filter house was designed for both GT configurations to house pre-filters and to provide a service area inside the duct to ease the replacement of pre-filters. Structural integrity and safety of the plants were also taken into account. The mentioned modifications eased the filter replacement process and reduced the number of shutdowns needed for filter replacement from 3 to only 1 per year which greatly improved the availability of the power plant.

## Introduction

With the rising demand for efficient energy conversion and power generation, enhancing the performance of gas turbines has become essential in meeting industrial requirements. The importance is further highlighted when considering the significant role that axial flow compressors play in achieving efficient operation of gas turbines. To improve the performance of axial flow compressors, several strategies have been developed such as alterations to the flow path, implementation of highly loaded blade designs with fewer compressor stages, and mitigation of flow separation from the blade surface. The primary objective of these approaches is to design compressors that exhibit high efficiency and stable operation under both design and off-design conditions and consequently, the gas turbines can achieve improved performance across a wide range of operations. Regarding compressor design process, the inverse design method serves as a new valuable approach, enabling the design team to achieve more efficient compressors based on the previous experience.

This integrated approach has led to notable advancements in design capabilities, enabling MAPNA Turbine to deliver cutting-edge solutions and stay at the forefront of the gas turbine industry.

# 4

## A Novel Approach towards Achieving Optimum Axial Compressor Design

Hasanlou, Sina  
Pakatchian, Mohammad  
Ranjbaran, Alireza

*MAPNA Turbine Engineering & Manufacturing Co.  
(TUGA)*

## Inverse Design Procedure

The aerodynamic design of compressors involves various factors due to the complicated nature of the flow. Many of these factors are associated with the overall geometry and limitations of the compressor such as flow path, clearances at the unshrouded blade tips, and presence of inter-stage cavities. However, other factors such as blade flow separations (which are possible to be encountered in the required range of blade operations) are directly related to the employed blade design technology. Blade flow separations can occur under specific operating conditions and have a significant impact on the efficiency and performance of the compressor. It is essential to carefully manage and minimize these physical phenomena through appropriate design techniques.

To develop relevant design procedures, Three-dimensional flow analysis is used to predict flow behavior in the flow path. However, despite the ability of numerical tools to identify undesirable phenomena such as flow separation, these tools are unable to determine the extent of geometrical changes required to mitigate these shortcomings and achieve the desired aerodynamic performance. Therefore, design optimization algorithms are employed to enhance the geometry design technology of compressor blades in pursuit of these performance objectives. Blade shape design and optimization methods can be classified into two categories: Direct Design and Inverse Design.

In the direct design method, the objective function is established within the limits of mechanical and geometrical constraints. The design process follows an iterative approach, optimizing the shape while considering these constraints. The defined objective function, through applying geometrical changes and evaluating their effects, determines the required adjustments to the geometry in an iterative process. This iterative loop continues until the objective function reaches a minimum value, at which point the process is terminated.

As for the inverse design method, the blade geometry is designed based on predetermined aerodynamic quantities. Velocity or pressure distribution are two target parameters that can be used as input for the algorithm. This can be applied to several airfoil sections through the blade geometry.

The inverse design optimization method offers flexibility in its implementation, allowing for both iterative and non-iterative approaches. In the non-iterative approach, connection is made between the body's shape and the dependent variables in the governing equations. This means that the optimal body shape is determined alongside the flow variables, resulting in a simultaneous solution. However, the calculation process becomes more intricate as it involves solving a system of nonlinear equations, which may present challenges in achieving convergence. Nonlinear systems often exhibit complex behavior, such as multiple solutions or sensitivity to initial conditions, making it more difficult to find a stable and accurate solution.

On the other hand, the iterative design process includes separate computations for flow and geometry modifications. In the iterative approach, the process begins with an initial estimation of the geometry such as that of a standard airfoil. The pressure distribution over this initial geometry is calculated and compared to the target distribution to determine the deviation from the desired performance specifications. The geometry is then modified using an optimization algorithm to achieve the desired objectives. Subsequent simulations are performed with the updated geometry, and this iterative cycle continues until convergence is achieved.

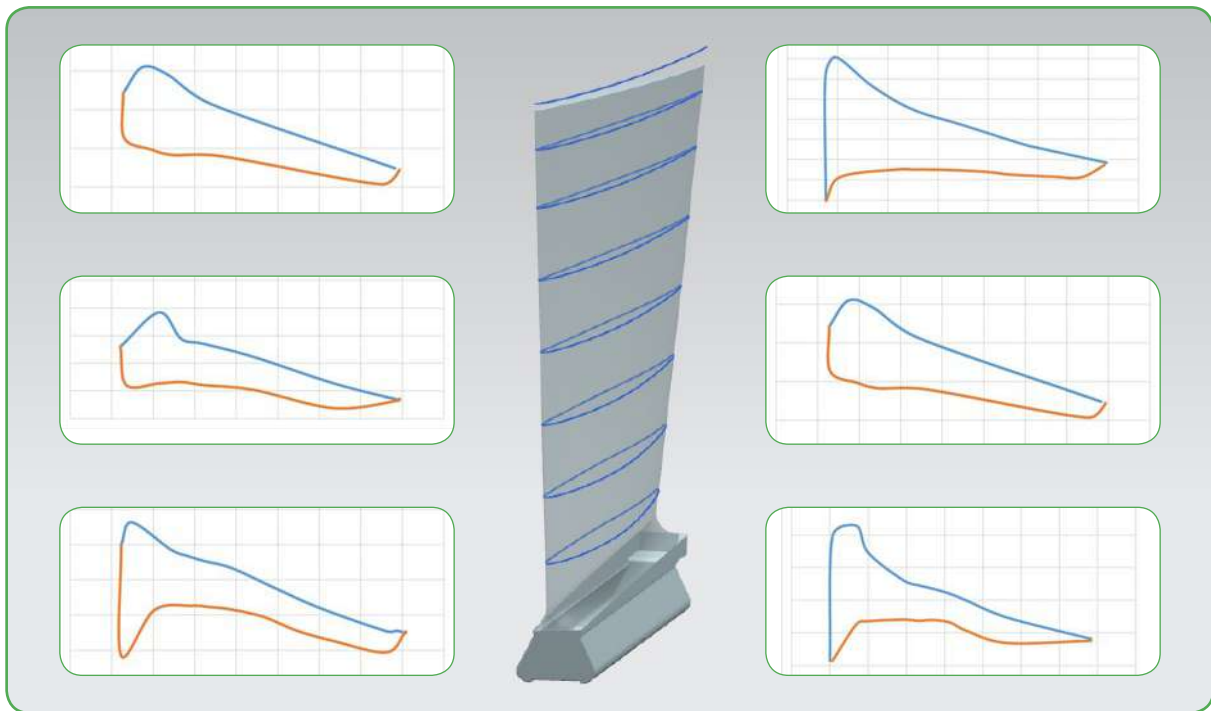


Figure 1- Pressure distribution over airfoil sections along a rotary blade

Figure 1 depicts the pressure distribution of sections, which may not be necessarily in their optimal state based on their boundary conditions. However, by employing an optimization approach based on the inverse design method, it is possible to achieve significant improvements by optimizing their pressure distribution.

In this design procedure, aerodynamic aspects are projected to a solid blade shape. Generally, flow properties along the boundaries of the blade geometry exhibit a nearly smooth distribution from the hub to the shroud. This smoothness has a direct impact on the distribution of aerodynamic quantities across the blade's 2D sections in the spanwise direction. Numerical evaluations have shown that maintaining a continuous distribution of aerodynamic quantities along the span significantly influences the smoothness of the blade surface. Consequently, the primary objective of the procedure is to achieve an aerodynamic distribution along the span that considers the continuity of these quantities. Furthermore, it is crucial to account for aerodynamic modifications that are necessary for both the design and off-design operation of gas turbines. Conducting preliminary analyses becomes imperative to ensure that the compressor operates within the desired range of performance. The combination of the aforementioned factors is summarized within the blade's 2D sections, which serve as the fundamental building blocks of a compressor. The pressure distribution across these sections is regarded as a significant aerodynamic parameter. Optimal pressure distribution in axial compressor cascades is achieved when the airfoils or blades in each stage are designed to strike a balance between the imposed losses and the recovery of total pressure. Moreover, the presence of shock phenomena can exert a substantial influence on the pressure distribution in axial compressor cascades. Shock waves arise when the air abruptly accelerates and exceeds a certain velocity threshold within the compressor. This abrupt change in velocity leads to a disruption in the pressure distribution across the blade, resulting in efficiency loss and potential blade damage. To achieve a suitable design optimization for cascade geometry using pressure distribution, the following points have to be taken into account: Presence and position of shock wave, the quality of the boundary layer and its potential for separation, as well as the pressure recovery across the cascade.

Generally, the iterative inverse design method offers the flexibility to study various flow regimes, including both subsonic and supersonic conditions. One of the notable advantages of this method is the simplicity of the governing equations, which makes them compatible with different flow solvers. However, one challenge in the iterative inverse design process is the computational time required to converge to a solution. To mitigate the downside and expedite the process, techniques such as utilizing databases and incorporating machine learning methods can be employed. These approaches help in reducing the computational burden and improving the efficiency of the design process.

By considering the above-mentioned parameters, the iterative approach is selected to be implemented in developing the inverse design method for axial compressor optimization.

## Implementation of the Inverse Design Method

This method serves as a robust design tool, allowing for precise adjustment of blade geometry based on specific operational conditions. The inverse design code has been developed as a sub-module within the compressor blade optimization package. This Python-based code facilitates the integration of optimization algorithm with the Star-CCM computational fluid dynamics (CFD) solver. This integration enables the method to be effectively utilized alongside other tools in an object-oriented manner, creating an integrated platform for compressor design. Furthermore, this integration opens up opportunities for leveraging powerful techniques such as database generation and machine learning within the Python environment. These techniques play crucial roles in generating an array of optimized geometries that are required at different sequences of compressor design and upgrade of MAPNA Turbine products.

As an important step, the parametrization of geometry is a crucial aspect in shape optimization as it determines the available degrees of freedom to achieve the desired geometry based on the selected pressure distribution. Efforts were made to implement effective methods that provide optimal flexibility in adapting the geometry. However, it is important to acknowledge that the process may encounter inherent errors. To address this, limitations were imposed to control and mitigate potential issues. For example, in certain cases, pressure discontinuities might arise. To manage such situations, artificial damping factors were introduced to alleviate any adverse effects. By carefully managing these limitations and applying appropriate control measures, the shape optimization process was carried out effectively. This ensured the attainment of more suitable geometries that align with the desired pressure distribution, thus enhancing the overall performance and efficiency of the design.

Moreover, in the realm of industrial design process, there are some other important factors, and the design process necessitates additional constraints stemming from geometrical limitations and mechanical considerations. When employing this method to upgrade the existing products, it becomes imperative to prioritize retrofitability. A pertinent example of this is the inherent limitations imposed by the available blade root dimensions, which can restrict the range of freedom in that particular area. Furthermore, mechanical factors must be carefully taken into account, encompassing aspects such as maximum thickness and its position, alongside undertaking static and dynamic analyses to ensure optimal performance.

To tackle these challenges, continuous advancements are being made in the domain of 2D connected shape optimizations, utilizing machine learning techniques. This ongoing development endeavors to strike a harmonious balance between retrofitability and adherence to mechanical considerations. By harnessing the power of machine learning, designers can elevate the design process, yielding optimized geometries that not only fulfill retrofitability requirements, but also satisfy the critical mechanical criteria.

To ensure a precise alignment between the parametrized 2D section geometries and the desired pressure distribution while minimizing any errors, the Elastic Surface Algorithm (ESA) was incorporated as a crucial component of the parametrization technique. The ESA method represents the airfoil surface as a flexible elastic beam, enabling iterative adjustments to its shape (see Figure 2). Initially, the airfoil or blade is assumed to be a flexible elastic beam. The flow field surrounding it is then solved using a flow solver, which allows for the calculation of the pressure distribution on both the suction and pressure sides of the blade. The difference between the target pressure distribution and the calculated pressure distribution drives the modification of the airfoil surface shape in each iteration. This iterative process continues until the stresses within the beam reach a state of equilibrium, meaning that the shape adjustments have converged to a satisfactory solution.

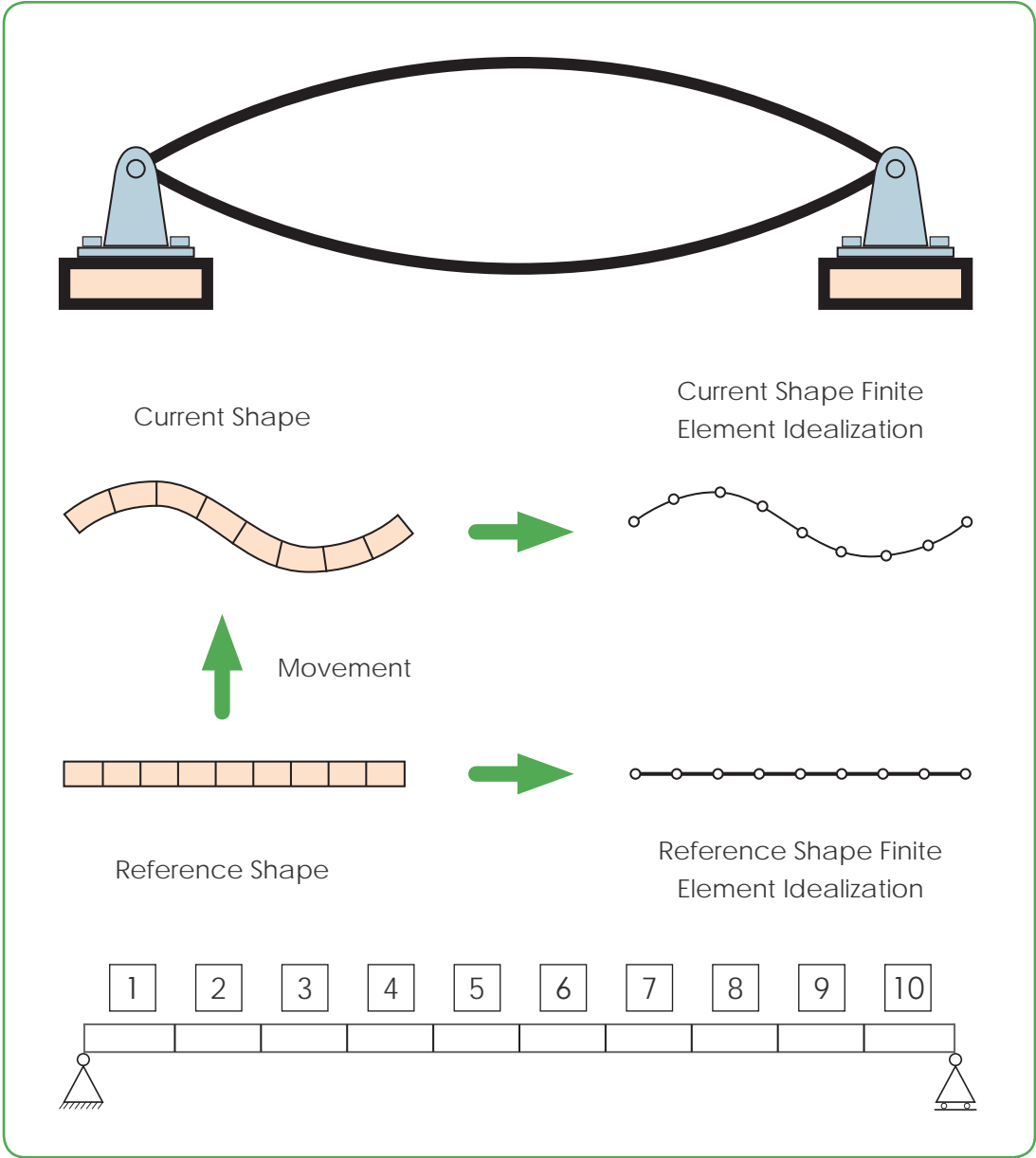


Figure 2- ESA parametrization technique

Figure 3 depicts the implementation of the optimization process using the inverse design algorithm. The design process begins by selecting an optimal pressure distribution and an initial standard airfoil geometry. Through numerical simulation of the initial geometry and extracting its pressure distribution, deviations from the target geometry on both the suction and pressure sides are evaluated. Subsequently, decisions are made regarding the pressure differences along both sides to generate the closest possible airfoil shapes, ensuring zero stress for the beam. This iterative process continues until the minimum error is achieved, resulting in an optimized airfoil geometry.

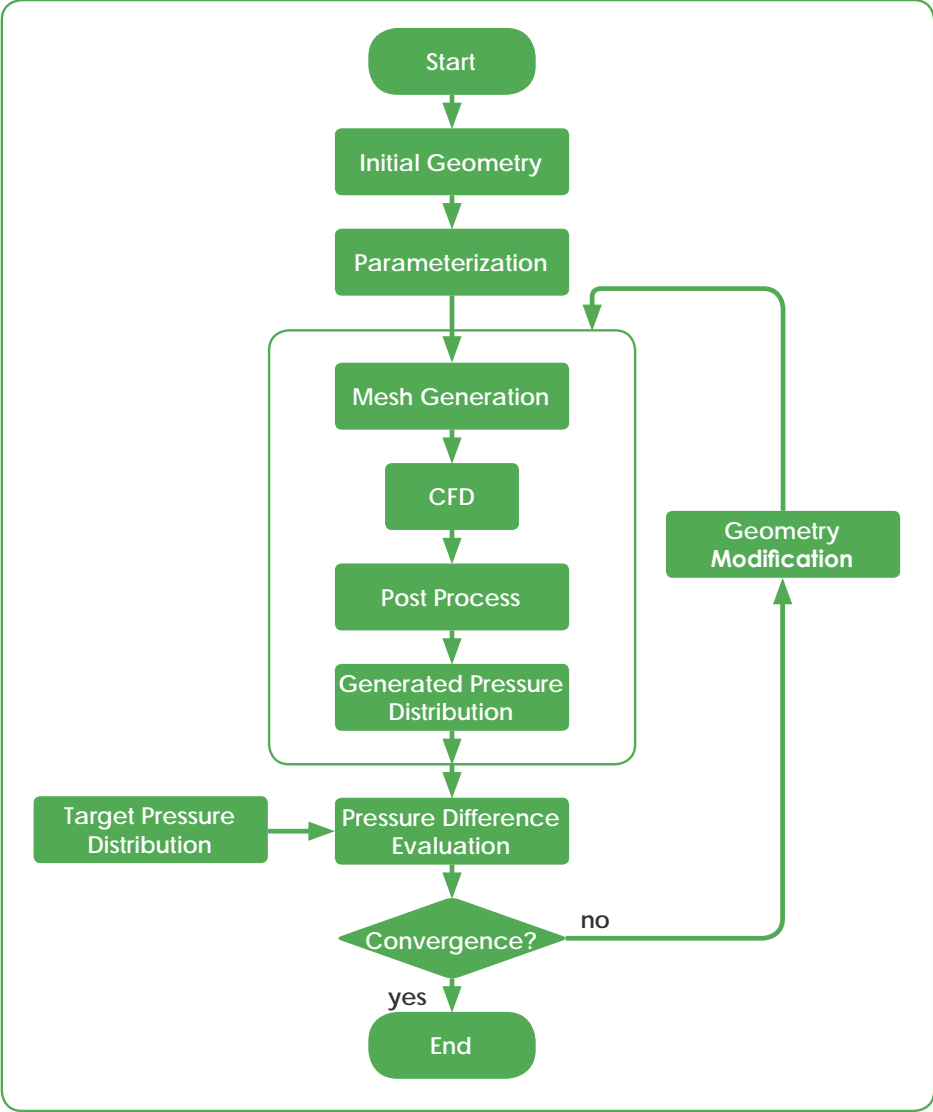


Figure 3- Inverse design flowchart

### An Example in Compressor Blades

The design process for a sample geometry from the third stage rotor of the MGT-70(3) GT's axial flow compressor is presented as a case study. The process began with extracting boundary condition data, which was crucial to ensure that the aerodynamic properties of the upstream and downstream of the target blade were properly accounted for. Due to blade root limitations and axial gaps, the generated geometries were constrained within predefined accessible geometric bands. This presented challenges in achieving the predefined pressure distribution, requiring the expertise of the design team to fine-tune the input data accordingly.

Figure 4 depicts the initial blade geometry and pressure loading indicating the starting point of the design process (dashed lines), along with the results after 150 iterations (red lines), as well as the target geometry and loading (green lines). By initiating an iterative process and carefully monitoring the generated pressure distributions, the target pressure distribution was eventually achieved and the solution converged within an acceptable error. It is worth noting that achieving convergence in the process requires careful control of the k factors, which relate to the adaptability of the pressure distribution and managing noisy environments. This implies that the convergence time and the quality of the generated geometry are two parameters that can have conflicting effects. To address this, customized coefficients were employed to fine-tune the convergence process.

It should be noted that the convergence process follows two different trends on the suction side and pressure side of the geometry, as illustrated in Figure 5.

The convergence rate can also vary for different blades and sections. This is primarily influenced by the flow regime (either subsonic or supersonic). Managing the shock position and controlling the discontinuities that arise when passing over the shock during the convergence process, can introduce instabilities. However, these issues can be addressed by fine-tuning the k factors, which helps to effectively control and mitigate the convergence challenges.

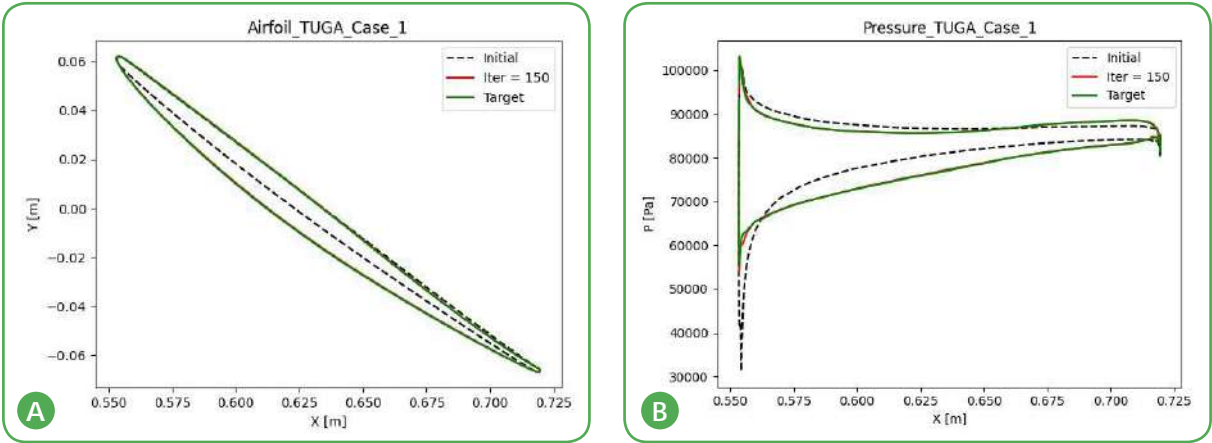


Figure 4: A: Initial geometry, target geometry, and calculated geometry in developed tools. B: Initial pressure loading, target pressure loading, and calculated pressure loading in developed tools after 150 iterations

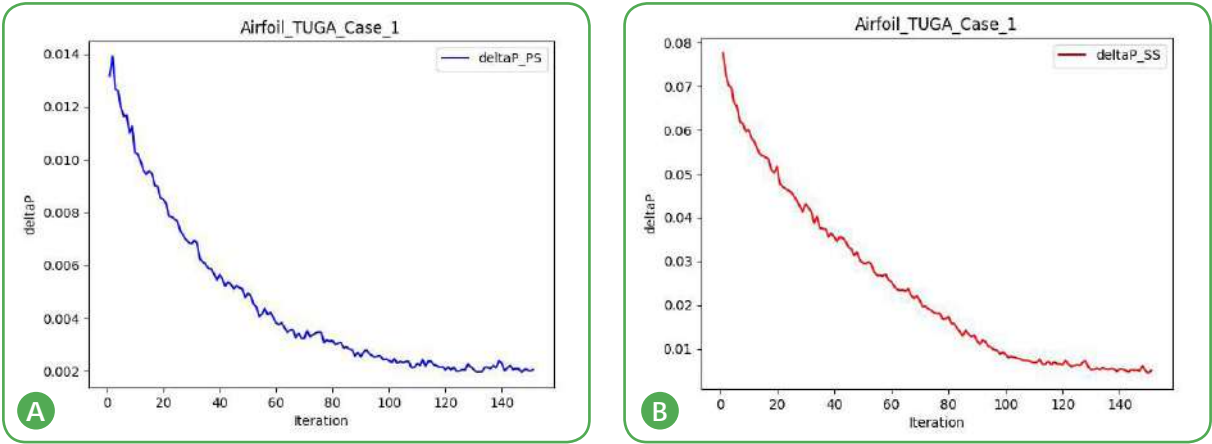


Figure 5: Pressure difference variation from start until the end in A: Pressure side and B: Suction side of the blade

## Concluding Remarks

The inverse design process in GT involves a blend of technical expertise and creative problem-solving skills. The design procedure and optimization can be considered as an art, as it requires a deep understanding of principles and the ability to translate conceptual ideas into practical designs. Through iterative refining and adjusting parameters, along with employing optimization techniques, engineers can achieve innovative and efficient solutions. The convergence of the process, with its iterative refinement and consideration of various design factors, highlights the complexity and artistry involved in achieving optimal engineering outcomes.

The inverse design procedure involves the utilization of optimization algorithms to adjust the blade geometry based on predetermined aerodynamic quantities, such as pressure or velocity distribution. It offers flexibility in implementation, allowing for both iterative and non-iterative approaches. However, computational time and convergence challenges can be encountered, which can be mitigated through techniques like utilizing databases and incorporating machine learning methods.

The implementation of the inverse design method, coupled with the integration of optimization algorithms and numerical software by MAPNA Turbine design office, represents a significant leap forward in the development of innovative compressor designs such as those incorporated in advanced H-class gas turbines. This integrated approach, supported by parametrization techniques such as Elastic Surface Algorithm, enables precise adjustments to the blade geometry based on specific operational conditions. By prioritizing retrofitability and considering mechanical considerations, the method ensures the generation of optimized geometries that enhance overall performance and efficiency.

## Introduction

Heavy-duty gas turbines constitute a significant portion of the power generation fleet all around the world. In 2021, the market size of industrial gas turbines surpassed US\$ 5.8B and it is anticipated to register over 5.8% Compound Annual Growth Rate (CAGR) between 2022 and 2030 [1]. To survive in this competitive market, manufacturers constantly strive for improved designs and machines with higher efficiencies and lower costs.

Axial flow compressor is one of the main components of an industrial gas turbine working on the basis of the Brayton cycle. The performance of axial compressors is affected by several factors such as ambient conditions, number of stages, operating conditions, blade specifications, etc. Since experimental procedures are significantly time-consuming and costly, numerical approaches are usually used to investigate these influences. Computational Fluid Dynamics (CFD) is broadly used for numerical investigation of axial compressors and various software have been developed to serve this purpose. However, numerical methods entail high computational costs due to the large domains to be analyzed.

Within this context, the R&D sector of MAPNA Turbine has introduced a new numerical simulation approach with focus on decrement in computational costs and time while maintaining the highest possible accuracy. In the following sections, the proposed approach is outlined and its accuracy is evaluated.

# 5

## An Innovative Method for Numerical Simulation of Axial Compressors

Nazari, Mohammad

MAPNA Turbine Engineering & Manufacturing Co.  
(TUGA)

## Proposed Approach

As pointed out in the last section, 3D numerical simulations are time-consuming procedures. To overcome this issue, some approaches have been proposed in the literature. For instance, it is possible to use 1D simulations with empirical correlations. However, these 1D methods lack the accuracy of 3D simulations and are not able to identify some of the fluid characteristics, which makes it difficult to get deep insight into the phenomena occurring in compressors. Similar disadvantages also exist in the case of 2D simulations.

To maintain accuracy, this study focused on the development of a 3D simulation with decreased computational costs. Within this framework, the 3D domain of the compressor was divided into 19 streamtubes. These streamtubes were specified using data obtained from a 3D simulation of the compressor. Instead of the whole geometry, the streamtube containing the meanline was then used to shrink the simulation domain as the fluid flow in this stream has the highest similarity to the actual flow. The boundary conditions at inlet and outlet of the compressor were set same as the simulation with complete geometry, but on the hub and shroud of blades and vanes (upper and lower walls), they were altered from no-slip wall condition to slip-wall condition.

Due to the reduction in simulation domain, the number of nodes and elements to be simulated was significantly reduced to approximately 5% of that of the complete geometry. This remarkably reduced the required simulation time, while maintaining the benefits of 3D simulation. Figure 1 illustrates the domains studied in complete 3D simulation and the proposed method.

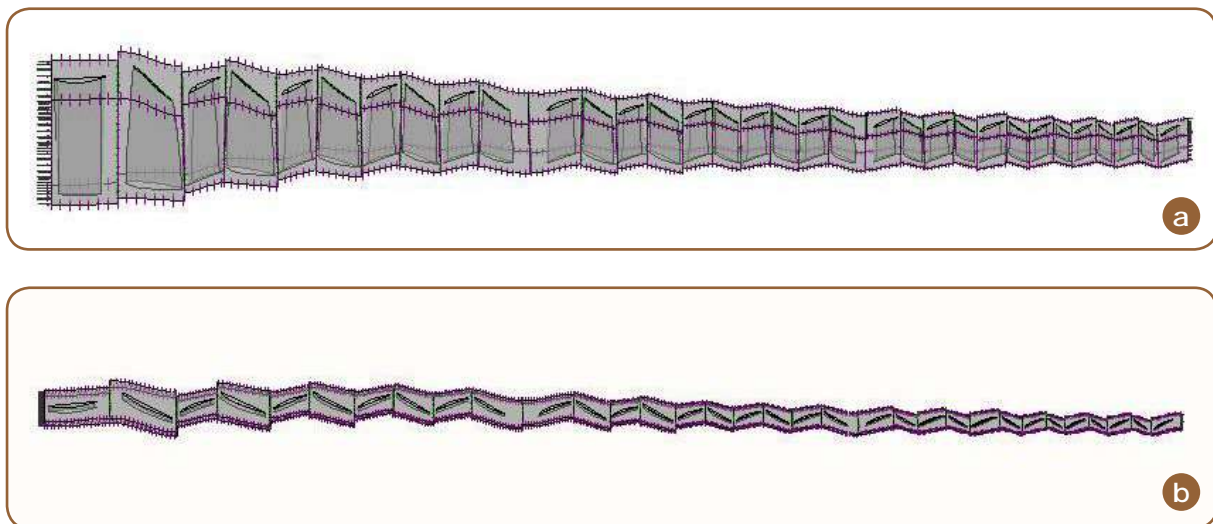


Figure 1 - Domains studied in a) complete 3D domain, and b) the streamtube containing the meanline (present method)

## Simulation Results

To evaluate the accuracy of the proposed approach, dimensionless pressure ratio and dimensionless efficiency of the compressor determined by the conventional method were compared with those calculated in the new approach for three corrected speeds 0.90, 0.95, and 1.05. Figures 2 and 3 show that the trend of data in complete geometry method is followed by that of the proposed approach. A deviation of less than 10% in the majority of the cases proves the proposed approach to be a reliable method considering the dramatic 95% reduction in computational costs.

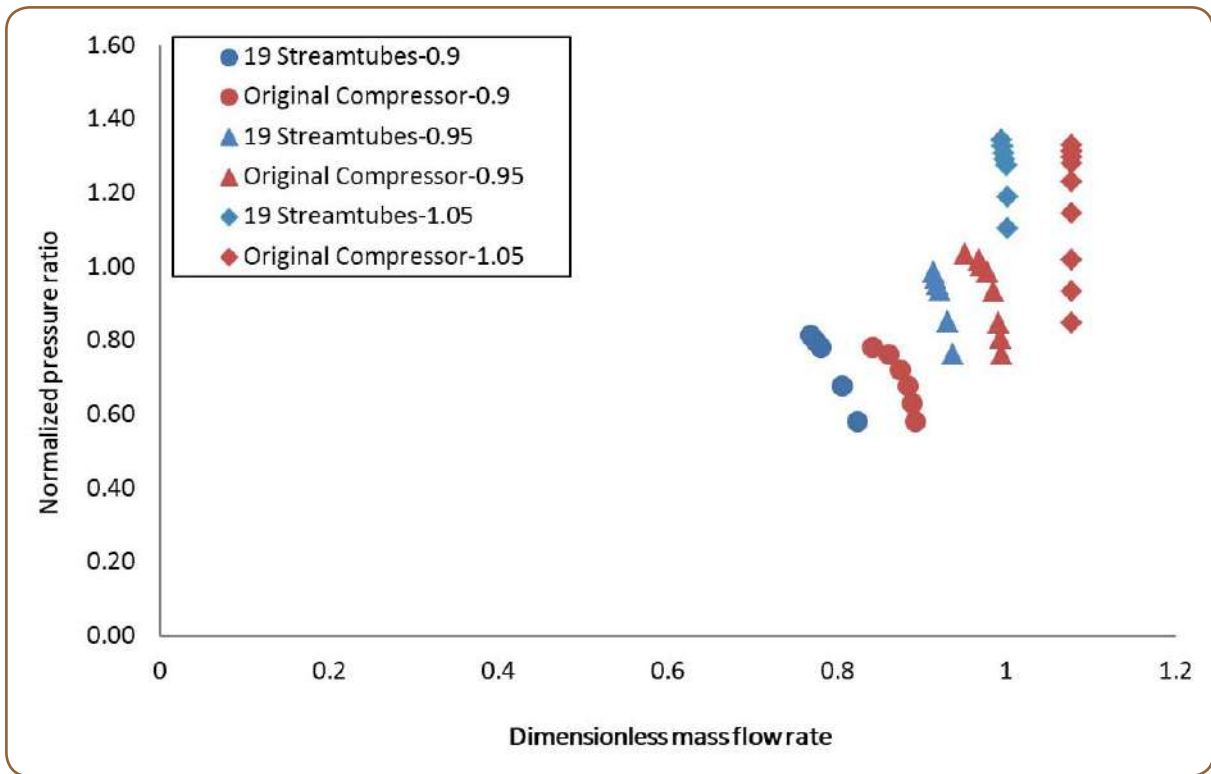


Figure 2- Normalized pressure ratio vs dimensionless mass flow rate

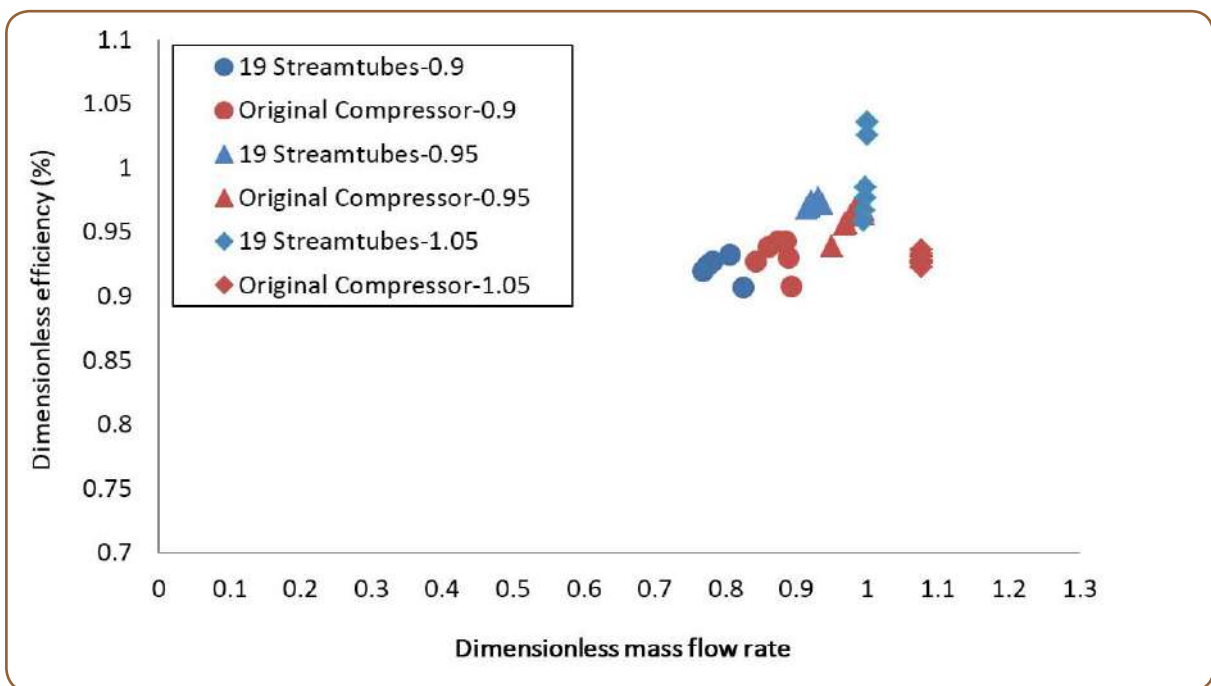


Figure 3- Dimensionless efficiency vs dimensionless mass flow rate

## Concluding Remarks

In this report, a novel simulation method for axial flow compressors was proposed by the R&D sector of MAPNA Turbine with significantly better performance compared to the conventional approaches. A comparison made between data obtained from the proposed approach and conventional techniques, successfully validated the accuracy and reliability of the new method. The introduced method significantly reduces computational costs and saves a considerable amount of time in the design and optimization of axial compressors. Additional efforts such as evaluation of different numbers of streamtubes and employment of particular streamtubes depending on the operating conditions of compressors can be made to further enhance the performance of this method.

## References

- [1] Industrial Gas Turbine Market n.d. <https://www.gminsights.com/industry-analysis/industrial-gas-turbine-market>.





**Head Office:**

231 Mirdamad Ave. Tehran, I.R.Iran.

P.O.Box: 15875-5643

Tel: +98 (21) 22908581

Fax: +98 (21) 22908654

**Factory:**

Mapna blvd., Fardis, Karaj, I.R.Iran.

Post code: 31676-43594

Tel: +98 (26) 36630010

Fax: +98 (26) 36612734

[www.mapnaturbine.com](http://www.mapnaturbine.com)

[tr@mapnaturbine.com](mailto:tr@mapnaturbine.com)

© MAPNA Group 2023

The technical and other data contained in this Technical Review is provided for information only and may not apply in all cases.